33rd Annual International Conference of the IEEE EMBS
Boston, Massachusetts USA, August 30 - September 3, 2011

Design and Simulation of Printed Spiral Coil used in Wireless Power Transmission Systems for Implant Medical Devices

Wei Wu, *Member, IEEE*, and Qiang Fang, *Member, IEEE*

***Abstract*—Printed Spiral Coil (PSC) is a coil antenna for near-field wireless power transmission to the next generation implant medical devices. PSC for implant medical device should be power efficient and low electromagnetic radiation to human tissues. We utilized a physical model of printed spiral coil and applied our algorithm to design PSC operating at 13.56 MHz. Numerical and electromagnetic simulation of power transfer efficiency of PSC in air medium is 77.5% and 71.1%, respectively. The simulation results show that the printed spiral coil which is optimized for air will keep 15.2% power transfer efficiency in human subcutaneous tissues. In addition, the Specific Absorption Ratio (SAR) for this coil antenna in subcutaneous at 13.56 MHz is below 1.6 W/Kg, which suggests this coil is implantable safe based on IEEE C95.1 safety guideline.**

I. Introduction

With the rapid development of microelectronics in recent decades, high performance implantable medical devices in modern health care has become increasingly important. Compared with other medical devices, implanted medical devices have the advantages of small size, light weight, more comfortable to wear, and they are directly within the organs or tissues of patients. As a result, treatments and diagnostic effects are more pronounced [1].

Wireless transmission system is the interface of implant medical devices to the outside world. Inductive wireless power transmission is the most common near field power coupling technique for implant medical devices. So far, most coils have been fabricated with litz wires by using sophisticated winding machinery [2]. Each time the winding coil could not guarantee the same merit. Besides, the size of winding coil is relatively large, which might not meet specific applications that have strict limits on the size of implants (such as bionic eye). Compared with traditional winding coil, printed spiral coil (PSC) has the following advantages —Firstly, design procedure of PSC is more convenient and the performance of coil can be optimized by adjusting its geometric parameters. Secondly, patient would feel more comfortable because PSC can be fabricated on flexible dielectric substrate [3]. Thirdly, PSC would be fabricated in conjunction with signal processing circuits in the same chip, this is the so called system-on-chip (SOC). In a word, printed spiral coil is a good candidate for near-field wireless power transmission to the next generation implant medical devices.

In this paper, we present printed spiral coil which was designed for implantable purpose. The structure of this paper is organized as follows. Physical model of PSC is introduced in Section II. The optimizing algorithm of coil design as well as MATLAB (MathWorks, Natk, MA) numerical calculation results are presented in Section III. Electromagnetic simulation of coils and its thermal effect to human subcutaneous tissue are discussed in Section IV. Measurement results of PSC in air medium are given in Section V. The concluding remarks are provided in Section VI.

II. Physical Model of Printed Spiral Coil

Fig. 1 shows a square PSC and its lumped equivalent circuit. The inductance, parasitic resistance and parasitic capacitance of coil are determined by several geometries, such as number of turns $\boldsymbol{n}$, inner and outer diameters $\boldsymbol{d_{in}}$ and $\boldsymbol{d_{out}}$, line width $\boldsymbol{w}$ and spacing $\boldsymbol{s}$ of copper wire. In the following, a simplified physical model that reveals the relationship between PSC geometric parameters and its equivalent circuit components value is constructed.

A. Inductance

Eq. (1) from [4] is adopted to calculate the inductance of square coil.

$$L = \frac{1.27 \cdot \mu n^2 D_{avg}}{2}\left[In\left(\frac{2.07}{\varphi}\right) + 0.18\varphi + 0.13\varphi^2 \right] \qquad (1)$$

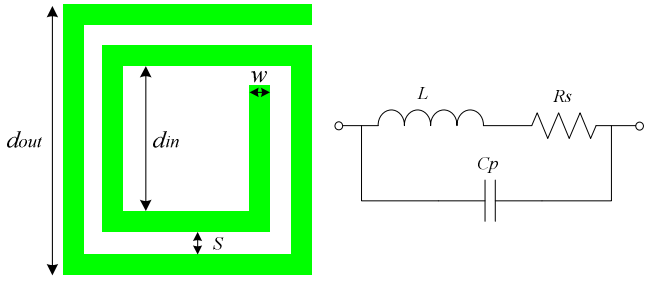

Fig. 1 Square coil and its lumped equivalent circuit

Where n is the number of turns, μ is the permeability, $D_{avg} = (d_{in} + d_{out})/2$. $\varphi = (d_{out} - d_{in})/(d_{out} + d_{in})$ is the fill factor.

This work was supported in part by the "Hundred Talents Program" of the Chinese Academy of Sciences Grant Y022021205.

Wei Wu is with Suzhou Institute of Biomedical Engineering and Technology, Chinese Academy of Sciences, Suzhou, Jiangsu 215163, P. R. China (email: wuw@sibet.ac.cn).

Qiang Fang is with Suzhou Institute of Biomedical Engineering and Technology, Chinese Academy of Sciences, P. R. China and the School of Electrical and Computer Engineering, RMIT University, Melbourne, Australia (email: johnqiangfang@gmail.com).

B. Parasitic Resistance

The parasitic resistance R_S is dominated by skin effect, and the related resistance is given by Eq. (2).

$$R_S = \frac{\rho \cdot length}{w \cdot \delta \cdot \left(1 - e^{-t/\delta}\right)} \tag{2}$$

$$length = 4nD_{avg} - n(0.5w + s) \tag{3}$$

$$\delta = \sqrt{\rho / (\pi f \mu)} \tag{4}$$

Where ρ, t, $length$ are the resistivity, thickness, length of the copper wire, respectively. δ is the skin depth [4].

C. Parasitic Capacitance

An empirical approach is used in finding the parasitic capacitance of the printed spiral coil [5]. A parallel plate parasitic capacitor forms between the spiral conductor sidewalls with air and FR4 substrate dielectrics. Therefore, the parasitic capacitor can be calculated from Eq. (5).

$$C_P = \frac{(\alpha\varepsilon_{air} + \beta\varepsilon_{FR4})\varepsilon_0 t L_{gap}}{s} \tag{5}$$

Where ε_{air} and ε_{FR4} are the relative permittivity of air and FR4 substrate. α and β are the empirical parameters, t is the thickness of copper wire. $L_{gap} = 4D_{avg}(n-1)$ is the length of spiral coil gap.

D. Power Transfer Efficiency

Fig. 2 shows an equivalent circuit diagram of inductive power transmission link, which operates like a transformer. L_1 is the primary coil resides outside the body and is usually driven by class E power amplifier. L_2 is the secondary coil implanted inside the body and its load is rectifier. R_s and C_p are the parasitic resistance and parasitic capacitance of coils, respectively. C_1 and C_2 are external tuning capacitors added to PSC.

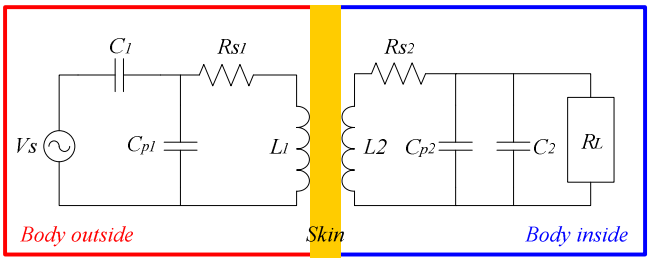

Fig. 2 Equivalent circuit diagram of inductive power transmission link

The coupling coefficient of the two coils is defined as $k = M / \sqrt{L_1 L_2}$, where L_1 and L_2 are self inductance of primary coil and secondary coil, and M is their mutual inductance. Eq. (6) is an approximate formula given in [6] to calculate the coupling coefficient of printed spiral coils in RFID.

$$k \approx \frac{r_1^2 r_2^2}{\sqrt{r_1 r_2}\left(\sqrt{D^2 + \max(r_1, r_2)^2}^3\right)} \tag{6}$$

Where r_1, r_2, D are the radius and distance of the two coils.

The highest power transfer efficiency η_{PSC} can be achieved when both coils are tuned at carrier frequency, η_{PSC} can be calculated from Eq. (7) given in [7],

$$\eta_{PSC} = \frac{k^2 Q_1 Q_{2p}}{1 + k^2 Q_1 Q_{2p}} \cdot \frac{Q_2}{Q_2 + Q_L} \tag{7}$$

Where $Q_{2p} = Q_2 Q_L / (Q_2 + Q_L)$. $Q_L \approx 2\pi f R_L C_2$ is the loaded quality factor of the secondary coil, $Q_1 = 2\pi f R_{S1} / L_1$, $Q_2 = 2\pi f R_{S2} / L_2$ are the unloaded quality factors of primary and secondary coil, respectively.

III. OPTIMIZATION OF PRINTED SPIRAL COIL

The efficiency of inductive power transmission link is low due to electromagnetic wave reflection at the air-skin interface and heat dissipation effect inside the tissues. So geometric parameters of printed spiral coil need to be optimized to maximum power transfer efficiency. Independent variables include number of turns ***n***, inner diameter $\boldsymbol{d_{in}}$, copper line width ***w***, line spacing ***s***. We swept these parameters to find the optimal values.

Table I summarizes the optimal geometries and numerical calculation results with MATLAB (MathWorks, Natk, MA). The size of secondary coil (implant coil) is 10×10 mm^2 and the coupling distance between coils is 10 mm. The power loss within human tissue can be low if the operating frequency of power carrier is below 20 MHz [8], we choose 13.56 MHz to be compatible with RFID (radio frequency identification) standards.

TABLE I
OPTIMAL GEOMETRIES AND SIMULATION RESULTS OF PRINTED SPIRAL COIL

Symbol	Parameter Name	Value
d_{i1}	Inner diameter of PSC1*	8 mm
d_{i2}	Inner diameter of PSC2*	6 mm
s_1	Copper line spacing of PSC1	250 μm
s_2	Copper line spacing of PSC2	150 μm
w_1	Copper line width of PSC1	2800 μm
w_2	Copper line width of PSC2	150 μm
n_1	Turns of PSC1	3
n_2	Turns of PSC2	7
L_1	Inductance of PSC1	0.18 μH
L_2	Inductance of PSC2	0.68 μH
R_{s1}	Parasitic resistance of PSC1	0.077 Ω
R_{s2}	Parasitic resistance of PSC2	1.607 Ω
C_{P1}	Parasitic capacitance of PSC1	0.54 pF
C_{P2}	Parasitic capacitance of PSC2	1.26 pF
SRF_1	Self resonance frequency of PSC1	509.2 MHz
SRF_2	Self resonance frequency of PSC2	171.9 MHz
k	Coupling coefficient	0.133
η_{PSC}	Power transfer efficiency	77.5%

*Primary coil and secondary coil are denoted by PSC1 and PSC2, respectively. Load resistance R_L=500 Ω, the distance between coils pair is 10 mm.

IV. ELECTROMAGNETIC SIMULATION

A. Simulation in Air Medium

At first, we simulated the pair of printed spiral coils in air medium. Fig. 3 shows the electromagnetic model of PSC constructed in CST (Computer Simulation Technology, AG, Germany). We used optimal geometries of coils given in TABLE I.

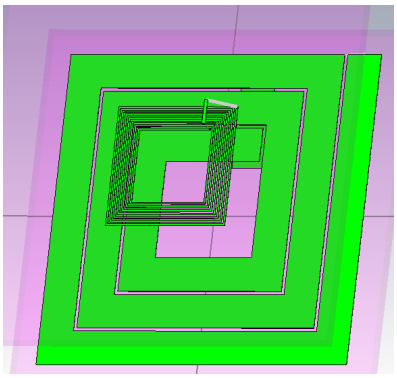

Fig. 3 Electromagnetic Model of Printed Spiral Coil in CST

We use CST to calculate the S-parameters of two-port network formed by primary and secondary coil. S-parameters are then converted to Z-parameters. The inductance and quality factor of individual PSC can be calculated by Z-parameters using the following formulas.

$$L_1=\frac{\mathrm{Im}(Z_{11})}{2\pi f},L_2=\frac{\mathrm{Im}(Z_{22})}{2\pi f},M=\frac{\mathrm{Im}(Z_{21})}{2\pi f}$$
$$Q_1=\frac{\mathrm{Im}(Z_{11})}{\mathrm{Re}(Z_{11})},Q_2=\frac{\mathrm{Im}(Z_{22})}{\mathrm{Re}(Z_{22})} \quad (8)$$

These parameters are then substituted in Eq. (7) to get the power transfer efficiency. The blue and red curve in Fig. 4 are the Matlab and CST simulation results of power transfer efficiency with frequency variation in air medium, respectively. The power transfer efficiency of coils pair operating at 13.56 MHz calculated by CST is 71.1%, slightly lower than the Matlab simulation result 77.5%. The variation mainly derives from the simplicity of physical model, which does not consider the secondary effects.

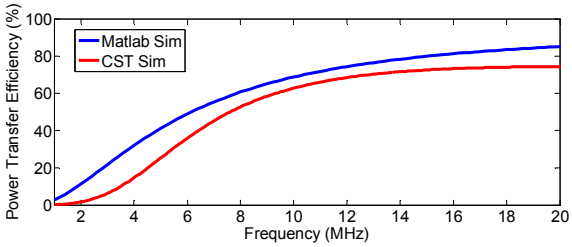

Fig. 4 Comparison of Matlab (blue) and CST (red) simulation results of power transfer efficiency with frequency variation in air medium

B. Simulation in Human Subcutaneous Tissue Medium

Assuming the medium between coil pairs are skin and fat tissues. Fig. 5 is the cross section of printed spiral coil with subcutaneous tissue, the distance between coils pair is 10 mm, the thickness ratio of skin and fat can be adjusted according to different circumstances. It is assumed that skin and fat occupy the same thickness (5 mm) in this paper. The dielectric properties of human subcutaneous tissues are frequency dependent. The relative permittivity and loss tangent of skin and fat at different frequency were calculated and imported into electromagnetic model using the parametric model developed in [9]-[11].

Fig. 5 Cross section of printed spiral coil with subcutaneous tissue

Fig. 6 is the CST electromagnetic simulation result of power transfer efficiency with frequency variation in subcutaneous tissue medium. The performance of PSC in subcutaneous tissue medium degenerates much worse than which in air medium. The peak power transfer efficiency is 15.2% and the frequency corresponding to the peak power transfer efficiency shifts to 8 MHz. This degradation derives from high water content and dielectric coefficient of human tissues, which would decrease the quality factor of PSC [12]. As a result, the resonance frequency shifts and peak power transfer efficiency decreases.

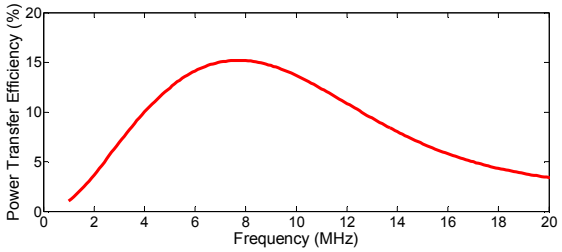

Fig. 6 CST electromagnetic simulation results of power transfer efficiency with frequency variation in subcutaneous tissue medium

Human subcutaneous tissues would absorb or reflect electromagnetic wave during wireless power transmission between the primary coil and secondary coil, and this would cause subcutaneous tissues heating. Specific absorption rate (SAR) is a measure of the rate at which energy is absorbed by the tissues when exposed to radio frequency electromagnetic field. It is defined as the power absorbed per mass of tissue and has units of W/kg [13]. Many international organizations have enacted safety guidelines of SAR. The IEEE C95.1 standard specifies the safety limit of SAR should below 1.6 W/kg taken over a volume containing a mass of 1 g tissue [14]. Fig. 7 is the CST simulation result, which gives SAR distribution in subcutaneous tissues at 13.56 MHz when apply 1 W power source. As can be seen from this figure, the high absorption rate occurrs mostly in the skin tissue near the primary coil. The SAR values are below 1.6 W/kg, which obeys the IEEE C95.1 safety limit.

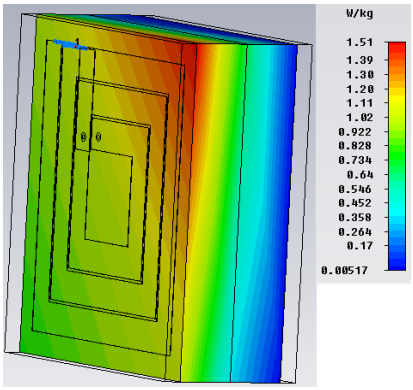

Fig. 7 Specific Absorption Rate (SAR) distribution in subcutaneous tissues at 13.56 MHz

V. MEASUREMENT RESULTS IN AIR MEDIUM

PSC was fabricated on FR4 substrate with the optimal geometries given in TABLE I. Fig. 8 gives the measurement result of peak to peak voltage of the secondary coil in air medium at different coupling distance while the stimulation sine wave (2 V peak to peak voltage at 13.56 MHz) is applied to the primary coil. As can be seen from this figure, output voltage of the secondary coil decreases with increasing coupling distance. Either increase the stimulation voltage of primary coil or place the pair of coils at a closer distance could achieve a higher output voltage.

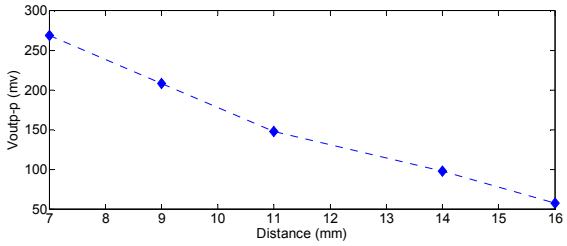

Fig. 8 Measurement result of peak to peak voltage of the secondary coil in air medium at different coupling distance

Fig. 9 is the measurement results of peak to peak voltage of the secondary coil with frequency variation in air medium. As can be seen from this figure, the maximum output voltage occurs at our specified operating frequency 13.56 MHz. The bell-shaped curve verifies the resonance-based principle of near-field wireless power transmission.

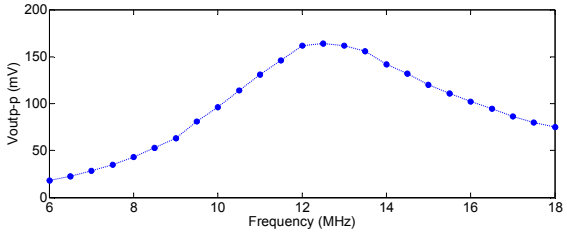

Fig. 9 Measurement result of peak to peak voltage of the secondary coil with frequency variation in air medium

VI. CONCLUSION

In this paper, a pair of printed spiral coil antennas used in wireless power transmission systems for implant medical devices is designed. Matlab numerical calculation and CST electromagnetic simulation indicate that the power transfer efficiency of PSC in air medium exceeds 70%, which verifies the rationality of the physical model. Simulation results of coils in human subcutaneous tissues shows that optimization of PSC in air medium has a significant degradation in performance in subcutaneous tissues, which is due to the high water content and dielectric coefficient in human tissues. The SAR distribution in subcutaneous tissues at 13.56 MHz was calculated and the SAR values are under the IEEE C95.1 safety limit. Preliminary experiments of PSC in air medium show that satisfactory power supply of implant medical devices can be achieved by increasing the stimulation power of primary coil or shortening the coupling distance between coil pairs when the PSCs are tuned at operating frequency. Future work will include the modification of the physical model, the development of an optimization algorithm for PSC in subcutaneous tissues medium, and the experimental verification of the designed PSC in a human subcutaneous tissue phantom.

REFERENCES

[1] Q. Fang, S. Y. Lee, H. Permana, K. Ghorbani, I. Cosic, "Developing a Wireless Implantable Body Sensor Network in MICS Band," IEEE Transaction on Information Technology in BioMedicine, accepted.

[2] Z. Yang, W. Liu, E. Basham, "Inductor modeling in wireless links for implantable electronics," IEEE Trans. Magn. Vol. 43, no. 10, pp. 3851-3860, Oct. 2007.

[3] R. R. Harrison, "Designing efficient inductive power links for implantable devices," IEEE Int. Symp. Circuits Syst., May 2007

[4] M. Zolog, D. Pitica, O. Pop. "Characterization of Spiral Planar Inductors Built on Printed Circuit Boards", 30th International Spring Seminar on Electronics Technology, May 2007.

[5] U. Jow and M. Ghovanloo, "Design and Optimization of Printed Spiral Coils for Efficient Transcutaneous Inductive Power Transmission," IEEE Trans. Biomed. Circuits Syst., vol. 1, no. 3, pp. 193-202, Sep. 2007

[6] K. A. Scott, "A Miniature Implantable Wireless Neural Stimulation System", Master thesis of Massachusetts Institute of Technology, Jun. 2006

[7] M. W. Baker and R. Sarpeshkar, "Feedback Analysis and Design of RF Power Links for Low-Power Bionic Systems", IEEE Trans. Biomed. Circuits Syst., vol. 1, no. 1, pp. 28-38, Mar. 2007

[8] P. Vaillancourt, A. Djemouai, J. F. Harvey and M. Sawan, "EM radiation behavior upon biological tissues in a radio-frequency power transfer link for a cortical visual implant," Proceedings of 19th Annual International Conference of the IEEE, vol. 6, pp. 2499-2502, Oct. 1997

[9] C. Gabriel, S. Gabriel, E. Corthout, "The dielectric properties of biological tissues: I. Literature survey", Phys. Med. Biol., vol. 41, pp. 2231-2249, Nov. 1996

[10] S. Gabriel, R. W Lau, and C. Gabriel, "The dielectric properties of biological tissues: II. Measurements in the frequency range 10 Hz to 20 GHz", Phys. Med. Biol., vol. 41, pp. 2251-2269, Nov. 1996

[11] S. Gabriel, R. W Lau, and C. Gabriel, "The dielectric properties of biological tissues: III. Parametric models for the dielectric spectrum of tissues", Phys. Med. Biol., vol. 41, pp. 2271-2293, Nov. 1996

[12] U. Jow and M. Ghovanloo, "Modeling and optimization of printed spiral coils in air, saline, and muscle tissue environments," IEEE Trans. Biomed. Circuits Syst., vol. 3, no. 5, pp. 339-347, Oct. 2009

[13] Jianming Jin, "Electromagnetic Analysis and Design in Magnetic Resonance Imaging," CRC Press, pp. 226, 1998

[14] IEEE, "IEEE Standard for Safety Levels with Respect to Human Exposure to Radio Frequency Electromagnetic Fields, 3 kHz to 300 GHz," 2002